

Investigating Correlations Between Functional Connectivity Disruption And Social Behavior Difficulties In Autism Spectrum Disorder

Shreya Karthik

Brown University, Providence, RI 02912, United States

ABSTRACT

Autism spectrum disorder (ASD) is a neurodevelopmental disorder characterized by impaired social behavior. Emerging evidence indicates that those with ASD exhibit disruption in neural networks supporting social behavior. This study investigated group and individual brain differences to identify the neural underpinnings of ASD. Resting-state functional magnetic resonance imaging data was obtained from the Autism Brain Imaging Data Exchange Initiative to perform whole-brain functional connectivity (FC) analysis, comparing ASD-affected brains to brains with typical development. Results showed lower FC in the ASD group among the following regions: left superior frontal gyrus, anterior cingulate gyrus, right posterior parahippocampal gyrus, left Heschl's gyrus, right planum polare, left and right precentral and right postcentral gyrus, left supracalcarine cortex, cuneus, right occipital pole, and cerebellum regions (vermis). These FC values were compared to measures of social behavior (the Social Responsiveness Scale (SRS) and the Social Communication Questionnaire (SCQ)). A negative correlation was found between the SRS awareness subscale score and connectivity of the right parahippocampal gyrus with the superior frontal gyrus, and a positive correlation was found between the SRS Mannerisms subscale and connectivity of Heschl's gyrus with the cerebellar vermis 1 2. Additionally, the SRS Cognition and Communication subscale scores were positively correlated to the connectivity of the left Heschl's gyrus with vermis 1 2. These results can be used to understand the neurological basis of ASD and determine an objective identification of ASD and the severity of social behavior impairment, leading to the development of effective individualized treatments for a better quality of life.

Keywords: Autism Spectrum Disorder; Functional Connectivity; Heterogeneity; Social Behavior; Neuroimaging

INTRODUCTION

Autism Spectrum Disorder (ASD) has a prevalence of about 1% globally (1–3). ASD is a group of neurodevelopmental disorders characterized by impairments in social communication, restrictive behaviors, and sensory processing abnormalities (4–18). These symptoms significantly affect educational, medical, and social outcomes (19–20). Earlier intervention can alter these numbers for a more positive life outlook; for this, an earlier and more accurate diagnosis must be facilitated (7).

Corresponding author: Shreya Karthik, E-mail: shreyakarthik319@gmail.com.

Copyright: © 2026 Shreya Karthik. This is an open access article distributed under the terms of the Creative Commons Attribution License, which permits unrestricted use, distribution, and reproduction in any medium, provided the original author and source are credited.

Accepted March 2 2026

<https://doi.org/10.70251/HYJR2348.427589>

Current ASD diagnosis relies on standardized behavioral assessments such as ADOS-2 and ADI-R (7, 21–22). However, these tools are limited when the examiner is not the primary diagnostician or the child has comorbidity with attention deficit hyperactivity disorder (ADHD) (23–24). These limitations may delay early diagnosis, highlighting the need for objective neurobiological biomarkers (25–26).

Focusing on the comparatively less explored underlying neurophysiological mechanisms can pave the way to identify biomarkers that enhance understanding of the causes of ASD, facilitating earlier and more precise diagnosis and intervention (7). Currently, though, most brain network studies in ASD have been limited to adults, though identifying neural abnormalities in childhood would be more meaningful (27). Therefore, this study aims to examine the underlying neural mechanisms of ASD earlier in life that are less prone to subjective limitations of the existing ASD diagnostic paradigm.

Resting-state functional magnetic resonance imaging (rs-fMRI) is an ideal measurement of neural connectivity for determining the neural circuitry of ASD. rs-fMRI can be obtained in 5-6 minutes, independent of task interpretation, while the participant lies still in the scanner, which is ideal for individuals with ASD with a wide range of cognitive abilities (7). It reveals the functional connectivity (FC) of brain regions, providing insight into the large-scale organization of the typical and atypical brain for comparison, which is ideal since recent studies have reached a universal agreement that ASD is associated with alterations in brain FC, including hypo-connectivity and hyper-connectivity (28). Though previous studies utilizing functional magnetic resonance imaging (fMRI) have not identified an objective biomarker of ASD, general trends have been identified (28).

Recent fMRI has demonstrated a consistent pattern of abnormal FC in those with ASD, including both hyper (enhanced) and hypo (diminished) connectivity (28). Typically, studies have found that children with ASD show hypoconnectivity while adolescents and adults with ASD demonstrate hyperconnectivity (29). More specifically, a systematic review and meta-analysis on task-based fMRI studies and a separate study found that the most reliable finding was a disturbance to the function of social brain regions in those with ASD (6, 30). The social brain includes prefrontal, temporal, limbic, and parietal regions implicated in social cognition (31–36) (Figure 1).

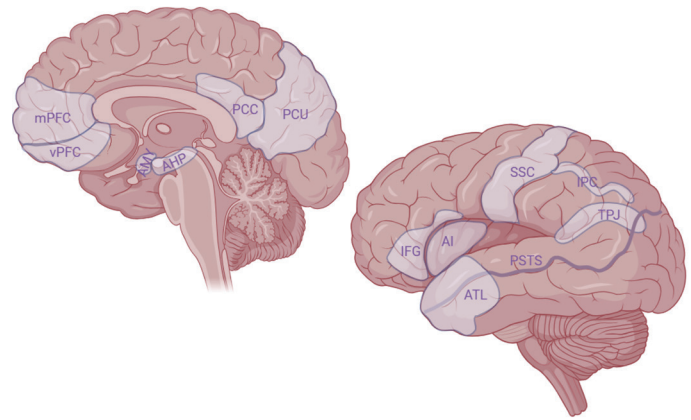


Figure 1. Sagittal cut and lateral view of the brain depicting social brain regions. mPFC, medial prefrontal cortex; vPFC, ventromedial prefrontal cortex; AMY, amygdala; AHP, anterior hippocampus; PCC, posterior cingulate cortex; PCU, precuneus; IFG, inferior frontal gyrus; AI, anterior insula; ATL, anterior temporal lobe; PSTS, posterior superior temporal sulcus; SSC, somatosensory cortex; IPC, intraparietal cortex; TPJ, temporal parietal junction. (Created with BioRender.com)

In children with ASD, the social brain has been shown to have reduced connectivity with the postcentral gyrus, precentral gyrus, supplementary motor area, paracentral lobule, medial cingulum cortex, and paracingulum gyri (37). Additionally, the FC of the amygdala is often disrupted in children with ASD, possibly leading to social behavior deficits (38). Similarly, the right fusiform gyrus and hippocampus have been shown to have reduced connectivity in children with ASD, which is also negatively correlated to ADOS severity scores (39).

There are also a considerable number of studies using the Autism Brain Imaging Data Exchange (ABIDE) to investigate functional connectivity disruptions in those with ASD. Prior ABIDE-based research has identified widespread connectivity alterations across cerebellar, temporal, and frontal regions (40–42). However, specific regions vary by study, as many of these investigations have focused on region-specific analyses. For example, two studies report aberrant FC between the cerebellum and cerebrum in individuals with ASD, including aforementioned regions such as the right fusiform gyrus, right superior temporal gyrus, left middle temporal gyrus, and inferior frontal gyrus, but also other novel regions, including the supramarginal gyrus and inferior parietal lobule. Anticorrelation has also been found between posterior and anterior regions of the brain with ASD, specifically within the paracingulate gyrus,

supramarginal gyrus, and middle temporal gyrus (42). In contrast to previous findings, however, another study reported limited FC differences in the somatosensory cortex (43).

Together, these results, both utilizing the ABIDE dataset and not, demonstrate that, despite a considerable body of knowledge and availability of a comprehensive database, though there are some overarching patterns in FC differences, the underlying neuromechanics of ASD have yet to be understood, and a biomarker has yet to be identified. There are most likely three reasons for this: (1) resting state studies each often only target a few regions at a time; (2) most studies do not account for the heterogeneity of ASD; and (3) research on youth with ASD is lacking in comparison to adults (27). With each study only examining a few regions at a time (e.g., only the cerebellum or only the somatosensory cortex, as seen in the aforementioned studies using the ABIDE dataset), it has provided a limited understanding of the full picture. Additionally, most studies focus on group differences using a traditional case-control approach, providing an understanding of only an average ASD patient. This leads to a failure to address the full heterogeneity seen on the spectrum despite the fact that understanding individual brain differences would be very helpful in widening understanding of the common neurological base of ASD alongside clinically heterogeneous symptoms (28, 44–45). Even studies that do compare FC disruptions to behavioral measures often focus on overall ASD symptomology or predefined brain regions, rather than a specific symptom category or the whole brain, which would be more helpful and allow for more detailed mapping. One such study using the ABIDE database was found showing specific correlations between cerebral FC and motor, executive, and socio-communicative functions (42). Similarly, a second ABIDE study found a relationship between social responsiveness and regions involved in the social preference of individuals with ASD (46). However, both these studies are limited by the fact that their results have not been reproduced, and they focus on predefined regions of the brain.

This study addresses the aforementioned gaps by examining adolescents (ages 12.1–16.9 years) using whole-brain functional connectivity (FC) analysis to (1) identify FC deficits in ASD through case-control comparison and (2) examine associations between FC alterations and social behavioral measures. This study hypothesized that regions implicated in social behavior, sensory processing, emotional regulation, attention, and behavioral control would exhibit hypoconnectivity in

ASD relative to typically developing (TD) controls, and that reduced connectivity would correlate with greater social impairment severity. Resting-state fMRI data from the ABIDE I dataset were used to perform a whole-brain between-subjects contrast (TD > ASD). Significant functional connectivity values were then correlated with Social Communication Questionnaire (SCQ) and Social Responsiveness Scale (SRS) scores to assess heterogeneity. By integrating whole-brain FC analysis with behavioral measures, this study aims to clarify the neural basis of social deficits in ASD and advance the identification of potential FC-based biomarkers.

METHODS AND MATERIALS

Participants and Data Source

As seen in Table 1, this study considers the data of thirty-five participants (ages 12.1-16.9 years), obtained from the ABIDE I database, The University of Leuven: Sample 2 (47). There are fifteen individuals with ASD, ages 12.1-16.8 years, and twenty individuals with typical development, ages 12.2-16.9 years (47). The sample comprised 23% females. The phenotypic and neuroimaging data of all thirty-five participants was used in the analysis, as there was no missing data or outliers. In the sample, the conserved exclusion criteria for both groups included the presence of a chronic

Table 1. Clinical information for all participants.

Characteristic	Mean ± SD	
	Autism Spectrum Disorder (n = 15)	Typical Development (n = 20)
Age at Scan	13.92 ± 1.311	14.34 ± 1.509
Verbal IQ	88.467 ± 20.262	114.7 ± 12.162
Performance IQ	100.2 ± 14.428	106.6 ± 8.281
SCQ Total	20.2 ± 8.728	3.65 ± 4.056
SRS Raw Total	91.067 ± 34.079	18.65 ± 14.737
SRS Awareness	11.067 ± 3.788	4.2 ± 3.019
SRS Cognition	17.333 ± 7.49	3.35 ± 3.281
SRS Communication	29.333 ± 12.827	5.4 ± 5.471
SRS Motivation	17.533 ± 6.978	3.6 ± 3.169
SRS Mannerisms	15.6 ± 6.345	2.35 ± 2.254

SRS = Social Responsiveness Scale; SCQ = Social Communication Questionnaire; SD = Standard Deviation.

medical illness, a metabolic disorder, or an abnormal conventional magnetic resonance imaging (MRI) or neurological examination. Participants in the ASD group were excluded if their ASD was associated with a genetic syndrome. Individuals in the ASD group were selected from a clinical sample of children with a previous diagnosis of ASD determined by a professionally accredited team based on the Diagnostic and Statistical Manual of Mental Disorders, Fourth Edition, Text Revision (DSM-IV-TR) criteria. Additionally, they had raw scores equal to or greater than 15 on the Social Communication Questionnaire (SCQ) and above 60 on the Social Responsiveness scale (SRS). The individuals in the TD group had no neurological or psychiatric diagnosis presently or in the past. Additionally, they reported no language problems.

Assessments

Verbal and personal IQ was calculated with an abbreviated version of the Dutch Wechsler Intelligence Scale for Children, Third Edition (48); handedness with the Dutch version of the Oldfield Handedness Questionnaire (49). The principal caregivers of all participants also completed the Social Communication Questionnaire (SCQ) and Social Responsiveness Scale (SRS) to confirm their placement in their corresponding group. The SCQ is a 40-item screening tool for ASD to evaluate typical behavioral symptomologies of ASD (50, 51). The SRS is also a screening tool for ASD, with 65 questions in total and 5 subscales of Restricted

Interests and Repetitive Behavior (Mannerisms), Social Awareness, Social Cognition, Social Communication, and Social Motivation (52).

Scan Acquisition

Participants were first trained before the scan session. Anatomical and rs-fMRI scans were obtained on a 3.0 Tesla Philips MR scanner (Best, The Netherlands) with an 8-channel phased-array head coil. Data was shared in the ABIDE I database regardless of movement/quality, and this study found no missing or abnormal data.

Preprocessing

All scan data was preprocessed before acquisition by the ABIDE Preprocessing Initiative. Briefly, this included motion correction, smoothing, skull stripping, high pass temporal filtering (0.01 - 0.1 Hz), nuisance signal removal, registering it to the standard Montreal Neurological Institute space (MNI-space), etc. Specific details can be found here (<http://preprocessed-connectomes-project.org/abide/Pipelines.html>) (53). Following preprocessing, resting state data was analyzed using the Functional Connectivity Toolbox (CONN toolbox).

Processing + Analysis

As indicated in Figure 2, resting state analysis was performed in the CONN toolbox, CONN: RRID SCR_009550, release 22 and SPM release 12.7771, a Matlab-based functional connectivity toolbox (54–56).

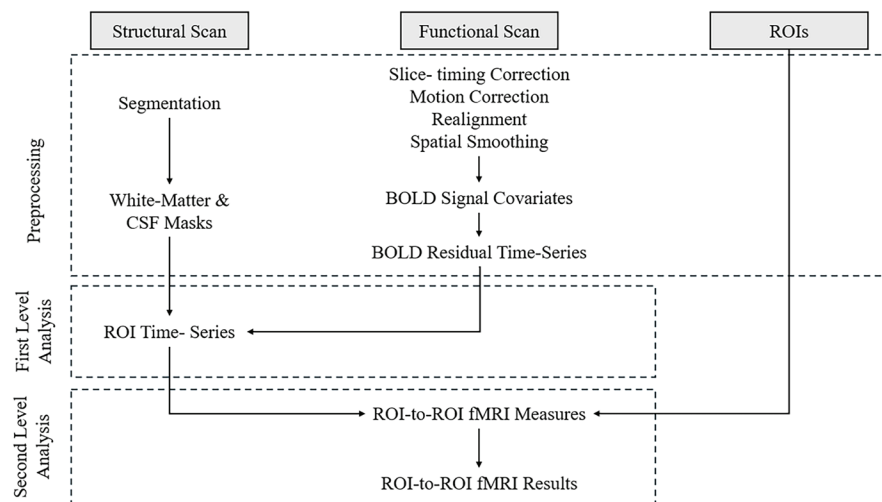


Figure 2. A Schematic representation of analysis steps. BOLD, blood oxygen level-dependent; CSF, cerebrospinal fluid; fMRI, functional magnetic resonance imaging; ROI, region of interest.

First, the functional acquisitions were prepared for analysis using the CONN toolbox preprocessing pipeline, with the following steps: motion correction, slice-timing correction, outlier detection, centering to (0,0,0) coordinates through translation, spatial smoothing with 8mm full-width half-maximum Gaussian kernel, and MNI-space normalization. The structural data was segmented (gray, white, cerebrospinal fluid), and normalized into MNI-space. More information can be found here: (<https://web.conn-toolbox.org/fmri-methods/preprocessing-pipeline>) (57).

Second, the setup pipeline computed the following steps: (1) imported data was checked for completeness (2) structural data was segmented into gray, white, and cerebrospinal fluid (CSF) tissue estimation (3) Conn imported conditions/covariates (4) Conn imported functional data (5) Conn imported region of interest (ROI) data (6) ROI data consistency was validated across all subjects (7) denoising variables for the next step were updated.

In addition, functional data were denoised using a standard denoising pipeline (58) including the regression of potential confounding effects characterized by white matter timeseries (5 CompCor noise components), CSF timeseries (5 CompCor noise components), session effects, and their first order derivatives (2 factors), and linear trends (2 factors) within each functional run, followed by bandpass frequency filtering of the Blood-Oxygen-Level-Dependent (BOLD) time series (59) between 0.008 Hz and 0.09 Hz. CompCor (60–61) noise components within white matter and CSF were estimated by computing the average BOLD signal as well as the largest principal components orthogonal to the BOLD average within each subject's eroded segmentation masks. From the number of noise terms included in this denoising strategy, the effective degrees of freedom of the BOLD signal after denoising were estimated to range from 64.2 to 64.2 (average 64.2) across all subjects (62). Details can be found here (<https://web.conn-toolbox.org/fmri-methods/denoising-pipeline>) (58).

In the first-level analysis SBC_01, seed-based connectivity maps (SBC) and ROI-to-ROI connectivity matrices (RRC) were estimated characterizing the patterns of functional connectivity with 164 HPC-ICA networks (56), and Harvard-Oxford atlas ROIs (63). Functional connectivity strength was represented by Fisher-transformed bivariate correlation coefficients from a weighted general linear model (weighted-GLM) (61), defined separately for each pair of seed and target areas, modeling the association between their BOLD

signal time series. In order to compensate for possible transient magnetization effects at the beginning of each run, individual scans were weighted by a step function convolved with an SPM canonical hemodynamic response function and rectified.

Group-level analyses were performed using a General Linear Model (GLM) (64). For each individual voxel, a separate GLM was estimated, with first-level connectivity measures at this voxel as dependent variables (one independent sample per subject and one measurement per task or experimental condition, if applicable), and groups or other subject-level identifiers as independent variables. Voxel-level hypotheses were evaluated using multivariate parametric statistics with random effects across subjects and sample covariance estimation across multiple measurements. Inferences were performed at the level of individual clusters (groups of contiguous voxels). Cluster-level inferences were based on parametric statistics from Gaussian Random Field theory (65–66). Results were thresholded using a combination of a cluster-forming probability < 0.001 ($p < 0.001$) voxel-level threshold, and a familywise corrected positive false discovery rate < 0.05 ($p\text{-FDR} < 0.05$) cluster-size threshold (67).

Using this data from the group analysis, a full brain ROI-to-ROI analysis was performed. Since adolescents with ASD often exhibit hypoconnectivity (29), a between-subjects contrast was applied to look for when the connectivity between two seeds in the TD group was greater than that in the ASD group (TD > ASD) with $p < 0.05$ significance threshold, FDR-corrected.

In a follow-up analysis, the connectivity values of the previously identified regions of the between-subjects contrast were extracted for each participant in the ASD group to explore whether any of these connections could serve as biomarkers of heterogeneity. Pearson product-moment correlations were computed, and the individual connectivity values for each region were compared to the individuals' scores on the SRS subscales and SCQ with and without age as a covariate, considering its effect on an adolescent's rapidly developing brain (34). This required comparing the FC value of each connection from the results of the group analysis to the total score of the SCQ and subscales scores of the SRS (Social Awareness, Social Cognition, Social Communication, Social Motivation, and Restricted Interests and Repetitive Behavior). A threshold of Pearson's r value < 0.4 was considered too weak to be discussed, a value of $0.8 > r \geq 0.4$ was moderately strong, and $1 > r \geq 0.8$ was a strong correlation. Only p -values < 0.05 were

considered significant. All statistical analyses were performed in JASP, version 0.18.3.0 (JASP Team, 2024).

RESULTS

The full-brain group-level analysis and between-subjects contrast (TD > ASD) yielded numerous results; this paper focuses on significant findings as shown in Table 2 and Figure 3. The data of all 35 participants was used throughout each stage of analysis without issue—no outliers or missing data was found, nor was data imputed.

Functional Connectivity in ASD v. TD

The whole-brain between-subjects contrast (TD > ASD) was conducted on the information that children with ASD exhibit hypoconnectivity compared to those with typical development (Uddin *et al.*, 2013). Our analysis revealed weakened FC between the following regions: right occipital pole and right posterior supramarginal gyrus (T(33) = 4.09, pFDR = 0.04); vermis 7 and right planum polare (T(33) = 4.21, pFDR = 0.03); vermis 1 2 and left Heschl’s gyrus (T(33) = 4.25, pFDR = 0.27); right posterior parahippocampal gyrus and left paracingulate gyrus (T(33) = 3.63, pFDR = 0.04), left superior frontal gyrus (T(33) = 3.54, pFDR = 0.04), anterior cingulate gyrus (T(33) = 3.66 pFDR = 0.04), right precentral gyrus (T(33) = 3.74, pFDR = 0.04), left precentral gyrus (T(33) = 3.23, pFDR = 0.05), right postcentral gyrus (T(33) = 3.28, pFDR = 0.05), left supracalcarine cortex (T(33) = 3.53,

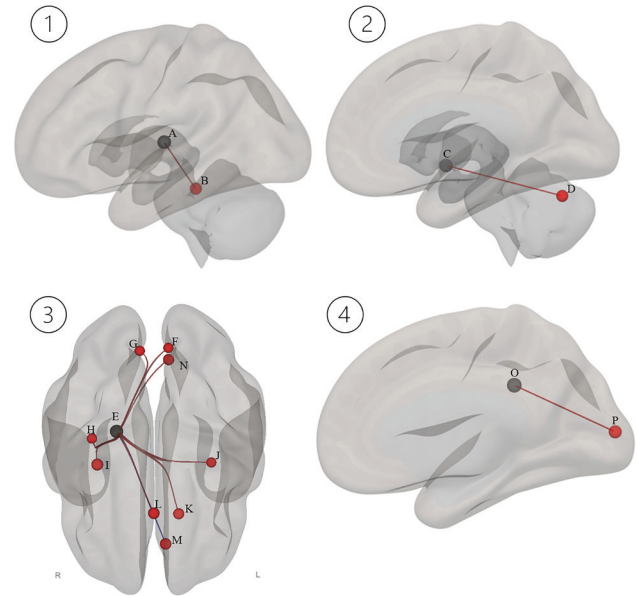


Figure 3. Four 3-dimensional depictions of significant connections from a whole-brain between-subjects contrast (TD > ASD). Each image has a different seed region in black. A = left Heschl’s gyrus; B = vermis 7; C = right planum polare; D = vermis 1 2; E = right posterior parahippocampal gyrus; F = left cuneal cortex; G = right cuneal cortex; H = right postcentral gyrus; I = right precentral gyrus; J = left precentral gyrus; K = left superior frontal gyrus; L = anterior cingulate gyrus; M = left paracingulate gyrus; N = left supracalcarine cortex; O = right posterior supramarginal gyrus; P = right occipital pole.

Table 2. Significant results from a whole-brain between-subjects contrast (TD > ASD)

Harvard-Oxford Atlas Regions		Statistic	p-unc	p-FDR
Seed ROI	Target ROI			
right posterior supramarginal gyrus	right occipital pole	T(33) = 4.09	0.0003	0.04
right planum polare	cerebellar vermis 7	T(33) = 4.21	0.0002	0.03
left Heschl’s gyrus	cerebellar vermis 1 2	T(33) = 4.25	0.0002	0.03
right posterior parahippocampal gyrus	left superior frontal gyrus	T(33) = 3.54	0.0012	0.04
	right postcentral gyrus	T(33) = 3.28	0.002	0.05
	anterior cingulate gyrus	T(33) = 3.66	0.0009	0.04
	left paracingulate gyrus	T(33) = 3.63	0.0009	0.04
	left supracalcarine cortex	T(33) = 3.53	0.001	0.04
	left cuneal cortex	T(33) = 3.19	0.003	0.05
	right cuneal cortex	T(33) = 3.25	0.003	0.05
	left precentral gyrus	T(33) = 3.23	0.003	0.05
	right precentral gyrus	T(33) = 3.74	0.0007	0.04

pFDR = 0.04), left cuneal cortex ($T(33) = 3.19$, pFDR = 0.05), and right cuneal cortex ($T(33) = 3.25$, pFDR = 0.05) It should also be mentioned that the correlations between all mentioned region pairs were strongly positively connected except for the left paracingulate gyrus and right posterior parahippocampal gyrus which exhibited strong negative correlation connectivity.

Correlations between Social Behavior Assessment Scores and Individual FC Measures

Because these connections were shown to be weakened in ASD, and therefore a differentiator of an ASD-affected brain from a TD brain, they were then utilized in a follow-up analysis to understand whether they could also be predictive of the heterogeneity of ASD, specifically looking at the severity of symptomatology. The individual connectivity values from the results of the contrast were compared to individuals’ total scores on the Social Communication Questionnaire and subscales scores on the Social Responsiveness Scale (Mannerisms, Social Awareness, Social Cognition, Social Communication, and Social Motivation) to explore the correlation between the connectivity strength of these regions and

symptom severity for those with ASD. Additionally, age was factored in as a covariate, considering its effect on an adolescent’s rapidly developing brain (34). Numerical results are shown in Tables 3 and 4 with graphical representations in Figure 4. Supporting the secondary hypothesis, a significant negative correlation was found between the SRS Awareness subscale score and connectivity of the right posterior parahippocampal gyrus with the left superior frontal gyrus ($r(35) = -0.58$, $p < 0.05$); also, a positive correlation was identified between the SRS Mannerisms score and connectivity of the left Heschl’s gyrus with vermis 1 2 ($r(35) = 0.683$, $p < 0.01$). Without age as a covariate, the positive correlation between the SRS Mannerisms score and connectivity of the left Heschl’s gyrus with vermis 1 2 was identified to be stronger ($r(35) = 0.719$, $p < 0.01$). Additionally, without age as a covariate, two new positive correlations were found: (1) the SRS Cognition score and connectivity of the left Heschl’s gyrus with vermis 1 2 ($r(35) = 0.557$, $p < 0.05$) and (2) the SRS Communication score and connectivity of the left Heschl’s gyrus with vermis 1 2 ($r(35) = 0.537$, $p < 0.05$).

Table 3. Results from Pearson product-moment correlations, comparing individual connectivity values from the results of the between-subjects contrast to individuals’ total scores on the Social Communication Questionnaire (SCQ) and subscales scores on the Social Communication Questionnaire (SRS) without age as a covariate.

Pearson Product-moment Correlations Comparing Individual Connectivity to individuals’ Scores on Behavioral Assessments without Age as a Covariate						
Functional Connectivity between Regions	SRS Awareness		SRS Cognition		SRS Communication	
	Pearson’s r	p value	Pearson’s r	p value	Pearson’s r	p value
pSMG r and OP r	-0.186	0.506	-0.189	0.499	-0.168	0.549
PP r and Ver7	-0.156	0.578	-0.316	0.251	-0.399	0.141
HG 1 and Ver12	0.432	0.108	0.557*	0.031	0.537*	0.039
pPaHC r and sFG1	-0.389	0.152	-0.139	0.622	-0.139	0.621
pPaHC r and PostCG r	0.054	0.849	0.154	0.584	0.238	0.393
pPaHC r and aCG r	0.091	0.747	0.414	0.125	0.359	0.189
pPaHC r and PCG 1	-0.374	0.170	-0.259	0.352	-0.204	0.466
pPaHC r and SCC 1	0.077	0.784	0.190	0.498	0.222	0.427
pPaHC r and CC 1	0.251	0.368	0.161	0.566	0.240	0.388
pPaHC r and CC r	0.423	0.117	0.307	0.266	0.307	0.266
pPaHC r and PreCG r	0.062	0.827	0.176	0.531	0.234	0.402
pPaHC r and PreCG 1	0.226	0.418	0.342	0.212	0.428	0.112

Continued Table 3. Results from Pearson product-moment correlations, comparing individual connectivity values from the results of the between-subjects contrast to individuals' total scores on the Social Communication Questionnaire (SCQ) and subscales scores on the Social Communication Questionnaire (SRS) without age as a covariate.

Functional Connectivity between Regions	SRS Motivation		SRS Mannerisms		SCQ Total	
	Pearson's r	p value	Pearson's r	p value	Pearson's r	p value
pSMG r and OP r	-0.341	0.214	-0.053	0.851	0.120	0.670
PP r and Ver7	-0.330	0.229	-0.345	0.208	-0.283	0.307
HG l and Ver12	0.164	0.560	0.719**	0.003	0.213	0.446
pPaHC r and sFG l	-0.225	0.420	-0.240	0.389	-0.035	0.9902
pPaHC r and PostCG r	0.031	0.913	0.077	0.786	-0.098	0.727
pPaHC r and aCG r	0.346	0.207	0.477	0.072	0.298	0.281
pPaHC r and PCG l	-0.141	0.617	-0.259	0.352	0.331	0.228
pPaHC r and SCC l	0.258	0.353	0.233	0.404	0.126	0.654
pPaHC r and CC l	-0.026	0.927	0.368	0.177	0.088	0.755
pPaHC r and CC r	0.239	0.390	0.437	0.103	-0.089	0.753
pPaHC r and PreCG r	0.033	0.908	0.169	0.548	0.012	0.965
pPaHC r and PreCG l	0.141	0.616	0.358	0.190	0.063	0.824

pSMG r = right posterior supramarginal gyrus; OP r = right occipital pole; PP r = right planum polare; Ver7 = vermis 7; HG l = left Heschl's gyrus; Ver12 = vermis 1 2; pPaHC r = right posterior parahippocampal gyrus; sFG l = left superior frontal gyrus; PostCG r = right postcentral gyrus; aCG r = right anterior cingulate gyrus; PCG l = left paracingulate gyrus; SCC l = left supracalcarine cortex; CC l = left cuneal cortex; CC r = right cuneal cortex; PreCG r = right precentral gyrus; PreCG l = left precentral gyrus. *p < 0.05, **p < 0.01, ***p < 0.001.

Table 4. Results from Pearson product-moment correlations, comparing individual connectivity values from the results of the between-subjects contrast to individuals' total scores on the Social Communication Questionnaire (SCQ) and subscales scores on the Social Communication Questionnaire (SRS) with age as a covariate.

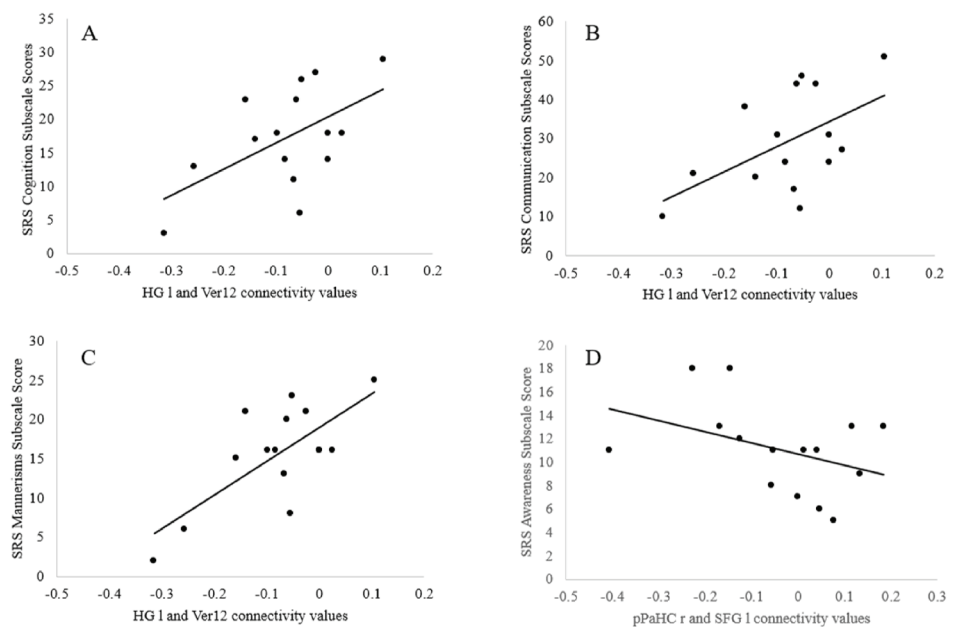
Pearson Product-moment Correlations Comparing Individual Connectivity to individuals' Scores on Behavioral Assessments with Age as a Covariate						
Functional Connectivity between Regions	SRS Awareness		SRS Cognition		SRS Communication	
	Pearson's r	p value	Pearson's r	p value	Pearson's r	p value
pSMGrand OP r	-0.193	0.508	-0.209	0.472	-0.187	0.522
PP r and Ver7	-0.042	0.887	-0.188	0.520	-0.286	0.321
HG l and Ver12	0.305	0.289	0.406	0.150	0.371	0.191
pPaHC r and sFG l	-0.58*	0.030	-0.374	0.187	-0.389	0.170
pPaHC r and PostCG r	-0.128	0.662	-0.086	0.769	0.011	0.970
pPaHC r and aCG r	0.074	0.802	0.448	0.108	0.388	0.170
pPaHC r and PCG l	-0.272	0.348	-0.085	0.774	-0.006	0.984
pPaHC r and SCC l	0.011	0.971	0.116	0.693	0.152	0.605
pPaHC r and CC l	0.189	0.519	0.062	0.834	0.154	0.600
pPaHC r and CC r	0.369	0.194	0.220	0.449	0.217	0.455
pPaHC r and PreCG r	-0.072	0.806	0.006	0.983	0.071	0.811
pPaHC r and PreCG l	0.020	0.947	0.075	0.800	0.182	0.533

Continued Table 4. Results from Pearson product-moment correlations, comparing individual connectivity values from the results of the between-subjects contrast to individuals' total scores on the Social Communication Questionnaire (SCQ) and subscales scores on the Social Communication Questionnaire (SRS) with age as a covariate.

Functional Connectivity between Regions	SRS Motivation		SRS Mannerisms		SCQ Total	
	Pearson's r	p value	Pearson's r	p value	Pearson's r	p value
pSMGrand OP r	-0.340	0.234	-0.049	0.868	0.123	0.674
PP r and Ver7	-0.316	0.271	-0.272	0.346	-0.259	0.371
HG l and Ver12	0.131	0.654	0.683**	0.007	0.176	0.546
pPaHC r and sFG l	-0.273	0.345	-0.377	0.184	-0.078	0.790
pPaHC r and PostCG r	-0.014	0.963	-0.066	0.822	-0.167	0.567
pPaHC r and aCG r	0.342	0.231	0.483	0.080	0.293	0.309
pPaHC r and PCG l	-0.112	0.704	-0.162	0.580	0.408	0.147
pPaHC r and SCC l	0.245	0.398	0.189	0.517	0.107	0.716
pPaHC r and CC l	-0.049	0.869	0.326	0.256	0.064	0.827
pPaHC r and CC r	0.222	0.445	0.393	0.165	-0.123	0.676
pPaHC r and PreCG r	-9.824×10^{-4}	0.997	0.073	0.804	-0.030	0.919
pPaHC r and PreCG l	0.102	0.728	0.232	0.425	-0.006	0.098

pSMG r = right posterior supramarginal gyrus; OP r = right occipital pole; PP r = right planum polare; Ver7 = vermis 7; HG l = left Heschl's gyrus; Ver12 = vermis 1 2; pPaHC r = right posterior parahippocampal gyrus; sFG l = left superior frontal gyrus; PostCG r = right postcentral gyrus; aCG r = right anterior cingulate gyrus; PCG l = left paracingulate gyrus; SCC l = left supracalcarine cortex; CC l = left cuneal cortex; CC r = right cuneal cortex; PreCG r = right precentral gyrus; PreCG l = left precentral gyrus. * $p < 0.05$, ** $p < 0.01$, *** $p < 0.001$.

Figure 4. Scatterplots A-D visually represent the significant Pearson product-moment correlations from comparing individual connectivity values from the results of the between-subjects contrast to individuals' total scores on the Social behavioral assessments. Graphs A and B shows positive correlations when age was not included as a covariate between the connectivity of the left Heschl's gyrus with vermis 1 2 and SRS subscale scores of Cognition ($r(35) = 0.557$, $p < 0.05$) and Communication ($r(35) = 0.537$, $p < 0.05$). Graph C demonstrates a positive correlation between the connectivity of the left Heschl's gyrus with vermis 1 2 and SRS Mannerisms score regardless of whether age was ($r(35) = 0.683$, $p < 0.01$) or was not ($r(35) = 0.719$, $p < 0.01$) included as a covariate. Finally, graph D shows a significant negative correlation between the SRS Awareness subscale score and connectivity of the right posterior parahippocampal gyrus with the left superior frontal gyrus ($r(35) = -0.58$, $p < 0.05$). HG l = left Heschl's gyrus; Ver12 = vermis 1 2; pPaHC r = right posterior parahippocampal gyrus; sFG l = left superior frontal gyrus; SRS = Social Responsiveness Scale.



DISCUSSION

This study examines a young population, conducting a whole-brain FC analysis with two objectives: first, identify deficits in FC in those with ASD with a traditional case-control analysis and second, appreciate the heterogeneity of ASD by comparing deficits in FC to scores on behavioral measures of social communication to investigate whether the FC irregularities can implicate the severity of social behavior difficulties in individuals with ASD. The hypothesis was that regions involved in aspects of social behavior, sensory sensitivity and integration, emotional processing, attention, and behavior inhibition would display interhypoconnectivity compared to a TD brain and that the FC of regions shown to have lower FC in those with ASD would be directly related to the severity of behavioral challenges experienced by those with ASD as measured by established behavioral assessments of social communication, awareness, cognition, motivation, and behavior. Evidence was found supporting both hypotheses.

The initial between-subjects contrast (TD > ASD) supported the first hypothesis by revealing significant hypoconnectivity between various brain regions in the ASD group, many of which are involved in aspects of social behavior, sensory sensitivity and integration, emotional processing, attention, and behavior inhibition. Specifically, the planum polare is located in the anterior temporal lobe, and the postcentral gyrus contains the primary somatosensory cortex, making them both a part of the social brain (33, 36, 68, 69). This supports past research indicating that individuals with ASD most commonly experience disruption to regions within their social brain (6, 30).

Also the result of hypoconnectivity between the vermis 1 2 (Ver 12) and the left Heschl's gyrus (HG l) was found in the ASD group. The HG is a part of the auditory cortex, involved in verbal language processing (70–73). The vermis is a region of the cerebellum involved in a variety of functions, including motor coordination in response to environmental stimuli (74), affective behavior (75), and emotional expression (76). In fact, abnormalities of the vermis lead to the least favorable outcomes for those with ASD, including pervasive developmental disorder and social deficits (77). The vermis has not been shown to have reduced connectivity with the HG in past literature, but these results support the first hypothesis. There was also a positive correlation found between the strength of this connectivity and individuals' scores on the social Mannerisms, Cognition,

and Awareness subscales of the SRS. Though results varied with the inclusion of age as a covariate, they imply that the stronger the connection between the HG l and Ver 12, the more difficulties individuals with ASD face in patterns of restricted and repetitive behaviors, as well as social cognition and awareness. This might not support the secondary hypothesis directly, but gives insight into the neural network of ASD and has the potential to serve as a biomarker of heterogeneity.

In this study, the right posterior parahippocampal gyrus (pPaHC r) exhibited hypoconnectivity with a variety of regions in the ASD group. The pPaHC is a region involved in connecting social context to understanding the emotions/tone of others (ex. sarcasm) (78–79). Additionally, it has been shown to be critical in visuospatial processing (70–86). Hypoconnectivity between any region and the pPaHC could therefore likely result in social interaction difficulties. In fact, the intensity of hypoconnectivity between the pPaHC r and left superior frontal gyrus (sFG l) was negatively correlated with the SRS social awareness subscale score when age was factored in as a covariate. A higher score on the subscale indicates greater difficulties in social awareness, so this negative correlation indicates that the strength of connectivity between the sFG l and pPaHC r is directly related to the severity of social awareness challenges in those with ASD. It should also be mentioned that, contrary to these results, a past study found heightened FC of the pPaHC; the discrepancy can be attributed to their older sample age and that their result highlights the full pPaHC rather than just the posterior division.

Overall, all the regions identified in the between-subjects contrast support the first hypothesis as they have involvement in social behavior, sensory sensitivity and integration, emotional processing, attention, and behavior inhibition. These results shed light on the homogenous neural underpinnings of ASD, aligning with past research showing that individuals with ASD experience disruptions to the function of social brain regions (6, 30). However, in past studies, these disruptions have been inconsistent due to the heterogeneity of individuals with ASD in each sample (7), leading to an incomplete understanding of the neural correlates of ASD and posing a barrier to identifying a diagnostic biomarker.

In this study, results directly correlating the strength FC of the pPaHC r and sFG l to behavioral measures support the second hypothesis, while the correlation between behavioral measures and the strength of FC between the HG and Ver 12 partially supports the

secondary hypothesis. These results provide insight into the heterogeneous neurological underpinnings of ASD, which can address the aforementioned inconsistencies seen in findings of past studies.

Moreover, the results could aid in the identification of biomarkers of ASD and biomarkers of heterogeneity of ASD, specifically for the severity of symptoms. Such an implication would allow for identified regions to be used as an objective diagnostic method for ASD, especially considering that the analysis of resting state fMRI has no subjectivity involved, like typically used behavioral assessments do. Whether understanding the neurological underpinnings of ASD or identification of biomarkers, these results can be augmented for the identification of ASD at earlier ages, and also measure the severity of symptoms to create individualized treatment plans that appreciate the heterogeneity of the spectrum and lead to better life stability outcomes.

Before this is achieved, more research needs to be conducted using the approach herein, continuing this pattern of analysis (whole-brain analysis and considering heterogeneity) with larger, more diverse samples. The sample used in this study was majority male, and though ASD is more prevalent in the male population, it is critical to conduct research that takes into account the effect that sex can have on the disorder to facilitate better and universal treatment plans. Additionally, to facilitate earlier diagnosis, even younger populations should be studied to characterize neural abnormalities near the age of 1, which is typically when behavioral measures are also used. Therefore, future recommendations include a larger sample size, with more females and younger subjects, continuing whole-brain analysis to obtain a comprehensive understanding of ASD neural changes, and considering heterogeneity in biomarker studies of ASD.

CONCLUSION

This study's purpose was to illuminate the neural underpinnings of ASD and its heterogeneity. This was accomplished through the analysis of functional connectivity and its comparison to social behavior measures.

Initial analysis of resting state fMRI data revealed significant hypoconnectivity between various brain regions in the ASD group that were not present in the TD group. Many of these regions are involved in social behavior, sensory sensitivity and integration, emotional processing, attention, and behavior inhibition, shedding

light on the homogenous neural underpinnings of ASD. This aligns with past research showing a general trend of disruptions to the function of social brain regions in individuals with ASD, though specific regions are difficult to pinpoint due to the diverse nature of symptomology in the spectrum. This study paved a path to alleviate this issue by comparing individuals' social behavior measure scores, representing the diversity of symptomology, to their functional connectivity values. Results correlating the strength FC of the pPaHC r and sFG l to behavioral measures provide insight into the heterogeneous neurological underpinnings of ASD, helping explain inconsistencies seen in findings on the common neural dysfunctions in individuals with ASD.

Future studies should maintain this pattern of whole-brain analysis to obtain a comprehensive understanding of ASD neural changes and consider heterogeneity in biomarker studies of ASD. Additionally, larger samples with more females and younger subjects are needed, as the sample used in this study was relatively small, comprised mostly of male teens. Such work will confirm the reproducibility of this study's findings and improve their generalizability.

Advancing understanding of FC differences in ASD will elucidate the neurobiological mechanisms underlying ASD related behavioral deficits, which can support the development of objective neural biomarker-based neuroimaging exams for the identification of ASD and its severity. Such tools can complement existing behavioral assessments and reduce subjectivity, enabling more precise diagnosis of ASD at a younger age. In response, treatment plans can be personalized on a behavioral and neurobiological level to reflect the diversity of ASD earlier in life to create better life outcomes for those affected. Ultimately, with continued validation in larger and younger cohorts, FC metrics can become clinically meaningful biomarkers that facilitate earlier diagnosis and individualized intervention.

CONFLICT OF INTEREST

The author declares that there are no conflicts of interest regarding the publication of this article.

REFERENCES

1. Kim YS, Leventhal BL, Koh YJ, Fombonne E, *et al.* Prevalence of autism spectrum disorders in a total population sample. *Am J Psychiatry*. 2011; 168 (9): 904-12. <https://doi.org/10.1176/appi.ajp.2011.10101532>

2. Nygren G, Cederlund M, Sandberg E, Gillstedt F, *et al.* The prevalence of autism spectrum disorders in toddlers: a population study of 2-year-old Swedish children. *J Autism Dev Disord.* 2012; 42 (7): 1491-7. <https://doi.org/10.1007/s10803-012-1488-x>, <https://doi.org/10.1007/s10803-011-1391-x>
3. Simonoff E. Autism spectrum disorder: prevalence and cause may be bound together. *Br J Psychiatry.* 2012; 201: 88-9. <https://doi.org/10.1192/bjp.bp.111.104703>
4. Dai Y, Zhang Y, Xu X, Zou X, *et al.* Shanghai Autism Early Development: an integrative Chinese ASD cohort. *Neurosci Bull.* 2022; 38 (12): 1603-7. <https://doi.org/10.1007/s12264-022-00904-y>
5. Fakhoury M. Autistic spectrum disorders: a review of clinical features, theories and diagnosis. *Int J Dev Neurosci.* 2015; 43: 70-7. <https://doi.org/10.1016/j.ijdevneu.2015.04.003>
6. Gotts SJ, Simmons WK, Milbury LA, Wallace GL, Cox RW, Martin A. Fractionation of social brain circuits in autism spectrum disorders. *Brain.* 2012; 135 (Pt 9): 2711-25. <https://doi.org/10.1093/brain/awsl60>
7. Lau WKW, Leung MK, Lau BWM. Resting-state abnormalities in autism spectrum disorders: a meta-analysis. *Sci Rep.* 2019; 9 (1): 3892. <https://doi.org/10.1038/s41598-019-40427-7>
8. Lord C, Elsabbagh M, Baird G, Veenstra-Vanderweele J. Autism spectrum disorder. *Lancet.* 2018;392(10146):508-20. [https://doi.org/10.1016/S0140-6736\(18\)31129-2](https://doi.org/10.1016/S0140-6736(18)31129-2)
9. Lundström S, Reichenberg A, Melke J, Råstam M, *et al.* Perceived child impairment and the 'autism epidemic'. *J Child Psychol Psychiatry.* 2022; 63 (5): 591-8. <https://doi.org/10.1111/jcpp.13497>
10. Zeng K, Kang J, Ouyang G, Li J, *et al.* Disrupted brain network in children with autism spectrum disorder. *Sci Rep.* 2017; 7 (1): 16253. <https://doi.org/10.1038/s41598-017-16440-z>
11. American Psychiatric Association. Diagnostic and statistical manual of mental disorders. 5th ed. Washington: APA; 2013. <https://doi.org/10.1176/appi.books.9780890425596>
12. Reindal L, Nærland T, Weidle B, Lydersen S, Andreassen OA, Sund AM. Structural and pragmatic language impairments in children evaluated for autism spectrum disorder (ASD). *J Autism Dev Disord.* 2023; 53 (2): 701-19. <https://doi.org/10.1007/s10803-020-04853-1>
13. Silleresi S, Prevost P, Zebib R, Bonnet-Brilhault F, Conte D, Tuller L. Identifying language and cognitive profiles in children with ASD via a cluster analysis exploration: implications for the new ICD-11. *Autism Res.* 2020; 13 (7): 1155-67. <https://doi.org/10.1002/aur.2268>
14. Chan AS, Han YMY, Leung WW, Leung C, Wong VC, Cheung MC. Abnormalities in the anterior cingulate cortex associated with attentional and inhibitory control deficits: a neurophysiological study on children with autism spectrum disorders. *Res Autism Spectr Disord.* 2011; 5 (1): 254-66. <https://doi.org/10.1016/j.rasd.2010.04.007>, <https://doi.org/10.1016/j.rasd.2010.04.005>
15. Baum SH, Stevenson RA, Wallace MT. Behavioral, perceptual, and neural alterations in sensory and multisensory function in autism spectrum disorder. *Prog Neurobiol.* 2015; 134: 140-60. <https://doi.org/10.1016/j.pneurobio.2015.09.007>
16. Iarocci G, McDonald J. Sensory integration and the perceptual experience of persons with autism. *J Autism Dev Disord.* 2006; 36 (1): 77-90. <https://doi.org/10.1007/s10803-005-0044-3>
17. Stevenson RA, Siemann JK, Schneider BC, Eberly HE, *et al.* Multisensory temporal integration in autism spectrum disorders. *J Neurosci.* 2014; 34 (3): 691-7. <https://doi.org/10.1523/JNEUROSCI.3615-13.2014>
18. Stevenson RA, Siemann JK, Woynaroski TG, Schneider BC, *et al.* Evidence for diminished multisensory integration in autism spectrum disorders. *J Autism Dev Disord.* 2014; 44 (12): 3161-7. <https://doi.org/10.1007/s10803-014-2179-6>
19. Farley MA, McMahon WM, Fombonne E, Jenson WR, *et al.* Twenty-year outcome for individuals with autism and average or near-average cognitive abilities. *Autism Res.* 2009; 2 (2): 109-18. <https://doi.org/10.1002/aur.69>
20. Steinhausen HC, Mohr Jensen C, Lauritsen MB. A systematic review and meta-analysis of the long-term overall outcome of autism spectrum disorders in adolescence and adulthood. *Acta Psychiatr Scand.* 2016; 133 (6): 445-52. <https://doi.org/10.1111/acps.12559>
21. Lord C, Rutter M, DiLavore PC, Risi S, Gotham K, Bishop S. Autism Diagnostic Observation Schedule. 2nd ed. Torrance: Western Psychological Services; 2012.
22. Lord C, Rutter M, Le Couteur A. Autism Diagnostic Interview-Revised: a revised version of a diagnostic interview for caregivers of individuals with possible pervasive developmental disorders. *J Autism Dev Disord.* 1994; 24 (5): 659-85. <https://doi.org/10.1007/BF02172145>
23. Charman T, Gotham K. Measurement issues: screening and diagnostic instruments for autism spectrum disorders - lessons from research and practise. *Child Adolesc Ment Health.* 2013; 18 (1): 52-63. <https://doi.org/10.1111/j.1475-3588.2012.00664.x>
24. Miodovnik A, Miodovnik A, Miodovnik A. Timing of the diagnosis of attention-deficit/hyperactivity disorder and autism spectrum disorder. *Pediatrics.* 2015; 136 (4): e830-7. <https://doi.org/10.1542/peds.2015-1502>

25. Dawson G, Jones EJ, Merkle K, Venema K, *et al.* Early behavioral intervention is associated with normalized brain activity in young children with autism. *J Am Acad Child Adolesc Psychiatry.* 2012; 51 (11): 1150-9. <https://doi.org/10.1016/j.jaac.2012.08.018>
26. Fernell E, Eriksson MA, Gillberg C. Early diagnosis of autism and impact on prognosis: a narrative review. *Clin Epidemiol.* 2013; 5: 33-43. <https://doi.org/10.2147/CLEP.S41714>
27. Doyle-Thomas KAR, Lee W, Foster NEV, Tryfon A, *et al.* Atypical functional brain connectivity during rest in autism spectrum disorders. *Ann Neurol.* 2015; 77 (5): 866-76. <https://doi.org/10.1002/ana.24391>
28. Shan X, Uddin LQ, Xiao J, He C, *et al.* Disentangling the individual-shared and individual-specific subspace of altered brain functional connectivity in autism spectrum disorder. *Biol Psychiatry.* 2024; 95 (9): 870-80. <https://doi.org/10.1016/j.biopsych.2023.09.012>
29. Uddin LQ, Supekar K, Menon V. Reconceptualizing functional brain connectivity in autism from a developmental perspective. *Front Hum Neurosci.* 2013; 7: 458. <https://doi.org/10.3389/fnhum.2013.00458>
30. Philip RCM, Dauvermann MR, Whalley HC, Baynham K, Lawrie SM, Stanfield AC. A systematic review and meta-analysis of the fMRI investigation of autism spectrum disorders. *Neurosci Biobehav Rev.* 2012; 36 (2): 901-42. <https://doi.org/10.1016/j.neubiorev.2011.10.008>
31. Brothers L. The social brain: a project for integrating primate behavior and neurophysiology in a new domain. *Foundations in Social Neuroscience.* 2002. <https://doi.org/10.7551/mitpress/3077.003.0029>
32. Frith CD, Frith U. Social cognition in humans. *Curr Biol.* 2007; 17 (16): R724-32. <https://doi.org/10.1016/j.cub.2007.05.068>
33. Adolphs R. The social brain: neural basis of social knowledge. *Annu Rev Psychol.* 2009; 60: 693-716. <https://doi.org/10.1146/annurev.psych.60.110707.163514>
34. Blakemore SJ. The social brain in adolescence. *Nat Rev Neurosci.* 2008; 9 (4): 267-77. <https://doi.org/10.1038/nrn2353>
35. Mitchell JP. Social psychology as a natural kind. *Trends Cogn Sci.* 2009; 13 (6): 246-51. <https://doi.org/10.1016/j.tics.2009.03.008>
36. Olson IR, Plotzker A, Ezzyat Y. The enigmatic temporal pole: a review of findings on social and emotional processing. *Brain.* 2007; 130 (Pt 7): 1718-31. <https://doi.org/10.1093/brain/awm052>
37. Wang Y, Zhang Y, Liu Y, Cui Z, *et al.* Social brain network of children with autism spectrum disorder: characterization of functional connectivity and potential association with stereotyped behavior. *Brain Sci.* 2023; 13 (2): 280. <https://doi.org/10.3390/brainsci13020280>
38. Liu X, Huber C, Bhatt DL, Bhatt D. Imbalance of laminar-specific excitatory and inhibitory circuits of the orbitofrontal cortex in autism. *Mol Autism.* 2020; 11 (1): 83. <https://doi.org/10.1186/s13229-020-00390-x>
39. Spera G, Genovese G, Cerasa A, Quattrone A, Sarica A. Evaluation of altered functional connections in male children with autism spectrum disorders on multiple-site data optimized with machine learning. *Front Psychiatry.* 2019; 10: 620. <https://doi.org/10.3389/fpsy.2019.00620>
40. Ramos TC, Balardin JB, Sato JR, Fujita A. Abnormal cortico-cerebellar functional connectivity in autism spectrum disorder. *Front Syst Neurosci.* 2018; 12: 74. <https://doi.org/10.3389/fnsys.2018.00074>
41. Hanaie R, Mohri I, Kagitani-Shimono K, Tachibana M, *et al.* Aberrant cerebellar-cerebral functional connectivity in children and adolescents with autism spectrum disorder. *Front Hum Neurosci.* 2018; 12: 454. <https://doi.org/10.3389/fnhum.2018.00454>
42. Heinsfeld AS, Franco AR, Craddock RC, Buchweitz A, Meneguzzi F. Identification of autism spectrum disorder using deep learning and the ABIDE dataset. *Neuroimage Clin.* 2018; 17: 16-23. <https://doi.org/10.1016/j.nicl.2017.08.017>
43. Cechmanek B, Greenough M, Wiley E, MacMaster FP, Lebel C. Somatosensory regions show limited functional connectivity differences in youth with autism spectrum disorder. *Brain Connect.* 2018; 8 (9): 558-66. <https://doi.org/10.1089/brain.2018.0614>
44. Tang S, Sun N, Floris DL, Zhang X, Di Martino A, Yeo BTT. Reconciling dimensional and categorical models of autism heterogeneity: a brain connectomics and behavioral study. *Biol Psychiatry.* 2020; 87 (12): 1071-82. <https://doi.org/10.1016/j.biopsych.2019.11.009>
45. Wolfers T, Beckmann CF, Hoogman M, Buitelaar JK, Franke B, Marquand AF. Individual differences v. the average patient: mapping the heterogeneity in ADHD using normative models. *Psychol Med.* 2020; 50 (2): 314-23. <https://doi.org/10.1017/S0033291719000084>
46. Deng S, Wang Y, Guan L, Li Y. Impaired effective functional connectivity in the social preference of children with autism spectrum disorder. *Front Neurosci.* 2024; 18: 1391191. <https://doi.org/10.3389/fnins.2024.1391191>
47. Di Martino A, Yan CG, Li Q, Denio E, *et al.* The autism brain imaging data exchange: towards a large-scale evaluation of the intrinsic brain architecture in autism. *Mol Psychiatry.* 2014; 19 (6): 659-67. <https://doi.org/10.1038/mp.2013.78>
48. Wechsler D. Wechsler Adult Intelligence Scale. 3rd ed. San Antonio: The Psychological Corporation; 1997. <https://doi.org/10.1037/t49755-000>

49. Oldfield RC. The assessment and analysis of handedness: the Edinburgh inventory. *Neuropsychologia*. 1971; 9 (1): 97-113. [https://doi.org/10.1016/0028-3932\(71\)90067-4](https://doi.org/10.1016/0028-3932(71)90067-4)
50. Eaves LC, Wingert HD, Ho HH, Mickelson EC. Screening for autism spectrum disorders with the social communication questionnaire. *J Dev Behav Pediatr*. 2006; 27 (2 Suppl): S95-103. <https://doi.org/10.1097/00004703-200604002-00007>
51. Marvin AR, Marvin DJ, Lipkin PH, Law JK. Analysis of Social Communication Questionnaire (SCQ) screening for children less than age 4. *Curr Dev Disord Rep*. 2017; 4 (4): 137-44. <https://doi.org/10.1007/s40474-017-0122-1>
52. Constantino JN. Social Responsiveness Scale. In: Volkmar F, editor. *Encyclopedia of autism spectrum disorders*. Cham: Springer; 2021; p4457-67. https://doi.org/10.1007/978-3-319-91280-6_296
53. Craddock C, Benhajali Y, Chu C, Chouinard F, et al. The Neuro Bureau Preprocessing Initiative: open sharing of preprocessed neuroimaging data and derivatives. *Neuroinformatics*. 2013.
54. Whitfield-Gabrieli S, Nieto-Castanon A. Conn: a functional connectivity toolbox for correlated and anticorrelated brain networks. *Brain Connect*. 2012; 2 (3): 125-41. <https://doi.org/10.1089/brain.2012.0073>
55. Nieto-Castanon A, Whitfield-Gabrieli S. CONN functional connectivity toolbox: RRID SCR_009550, release 22. Boston: Hilbert Press; 2022. <https://doi.org/10.56441/hilbertpress.2246.5840>
56. Friston KJ, Ashburner JT, Kiebel SJ, Nichols TE, Penny WD, editors. *Statistical parametric mapping: the analysis of functional brain images*. London: Academic Press; 2006.
57. Nieto-Castanon A. fMRI minimal preprocessing pipeline. In: *Handbook of functional connectivity magnetic resonance imaging methods in CONN*. Boston: Hilbert Press; 2020; p.3-16. <https://doi.org/10.56441/hilbertpress.2207.6599>
58. Nieto-Castanon A. fMRI denoising pipeline. In: *Handbook of functional connectivity magnetic resonance imaging methods in CONN*. Boston: Hilbert Press; 2020; p.17-25. <https://doi.org/10.56441/hilbertpress.2207.6600>
59. Hallquist MN, Hwang K, Luna B. The nuisance of nuisance regression: spectral misspecification in a common approach to resting-state fMRI preprocessing reintroduces noise and obscures functional connectivity. *Neuroimage*. 2013; 82: 208-25. <https://doi.org/10.1016/j.neuroimage.2013.05.116>
60. Behzadi Y, Restom K, Liao J, Liu TT. A component based noise correction method (CompCor) for BOLD and perfusion based fMRI. *Neuroimage*. 2007; 37 (1): 90-101. <https://doi.org/10.1016/j.neuroimage.2007.04.042>
61. Chai XJ, Castañón AN, Ongür D, Whitfield-Gabrieli S. Anticorrelations in resting state networks without global signal regression. *Neuroimage*. 2012; 59 (2): 1420-8. <https://doi.org/10.1016/j.neuroimage.2011.08.048>
62. Nieto-Castanon A. Preparing fMRI data for statistical analysis. ArXiv [Preprint]. 2022. Available from: <https://arxiv.org/abs/2210.13564>.
63. Desikan RS, Ségonne F, Fischl B, Quinn BT, et al. An automated labeling system for subdividing the human cerebral cortex on MRI scans into gyral based regions of interest. *Neuroimage*. 2006; 31 (3): 968-80. <https://doi.org/10.1016/j.neuroimage.2006.01.021>
64. Nieto-Castanon A. General linear model. In: *Handbook of functional connectivity magnetic resonance imaging methods in CONN*. Boston: Hilbert Press; 2020; p.63-82. <https://doi.org/10.56441/hilbertpress.2207.6602>
65. Worsley KJ, Marrett S, Neelin P, Vandal AC, Friston KJ, Evans AC. A unified statistical approach for determining significant signals in images of cerebral activation. *Hum Brain Mapp*. 1996; 4 (1): 58-73. [https://doi.org/10.1002/\(SICI\)1097-0193\(1996\)4:1<58::AID-HBM4>3.0.CO;2-O](https://doi.org/10.1002/(SICI)1097-0193(1996)4:1<58::AID-HBM4>3.0.CO;2-O)
66. Nieto-Castanon A. Cluster-level inferences. In: *Handbook of functional connectivity magnetic resonance imaging methods in CONN*. Boston: Hilbert Press; 2020; p.83-104. <https://doi.org/10.56441/hilbertpress.2207.6603>
67. Chumbley J, Worsley K, Flandin G, Friston K. Topological FDR for neuroimaging. *Neuroimage*. 2010; 49 (4): 3057-64. <https://doi.org/10.1016/j.neuroimage.2009.10.090>
68. DiGiuseppi J, Tadi P. Neuroanatomy, postcentral gyrus. In: *StatPearls*. Treasure Island: StatPearls Publishing; 2023.
69. Gage NM, Baars BJ. The brain. In: *Fundamentals of cognitive neuroscience*. 2nd ed. London: Academic Press; 2018; p.17-52. <https://doi.org/10.1016/B978-0-12-803813-0.00002-7>
70. Derey K, Valente G, de Gelder B, Formisano E. Opponent coding of sound location (azimuth) in planum temporale is robust to sound-level variations. *Cereb Cortex*. 2016; 26 (1): 450-64. <https://doi.org/10.1093/cercor/bhv269>
71. Khalighinejad B, Nagamine T, Mehta AD, Mesgarani N. Functional characterization of human Heschl's gyrus in response to natural speech. *Neuroimage*. 2021; 235: 118003. <https://doi.org/10.1016/j.neuroimage.2021.118003>
72. O'Connor K. Auditory processing in autism spectrum disorder: a review. *Neurosci Biobehav*

- Rev. 2012; 36 (2): 836-54. <https://doi.org/10.1016/j.neubiorev.2011.11.008>
73. Skipper JI, Small SL. fMRI studies of language. In: Encyclopedia of language and linguistics. 2nd ed. Oxford: Elsevier; 2006; p.496-511. <https://doi.org/10.1016/B0-08-044854-2/02399-3>
 74. Coffman KA, Dum RP, Strick PL. Cerebellar vermis is a target of projections from the motor areas in the cerebral cortex. *Proc Natl Acad Sci U S A*. 2011; 108 (38): 16068-73. <https://doi.org/10.1073/pnas.1107904108>
 75. Konczak J, Timmann D. The effect of damage to the cerebellum on sensorimotor and cognitive function in children and adolescents. *Neurosci Biobehav Rev*. 2007; 31 (8): 1101-13. <https://doi.org/10.1016/j.neubiorev.2007.04.014>
 76. Schmahmann JD. Disorders of the cerebellum: ataxia, dysmetria of thought, and the cerebellar cognitive affective syndrome. *J Neuropsychiatry Clin Neurosci*. 2004; 16 (3): 367-78. <https://doi.org/10.1176/jnp.16.3.367>
 77. Hampson DR, Blatt GJ. Autism spectrum disorders and neuropathology of the cerebellum. *Front Neurosci*. 2015; 9: 420. <https://doi.org/10.3389/fnins.2015.00420>
 78. Aminoff EM, Kveraga K, Bar M. The role of the parahippocampal cortex in cognition. *Trends Cogn Sci*. 2013; 17 (8): 379-90. <https://doi.org/10.1016/j.tics.2013.06.009>
 79. Harlalka V, Naik S, Bhatt P, Kiran S. Integration and segregation in autism spectrum disorders modulated by age, disease, and interaction: a graph theoretic study of intrinsic functional connectivity. *BioRxiv* [Preprint]. 2018. Available from: <https://www.biorxiv.org/content/10.1101/278846v1>. <https://doi.org/10.1101/278846>
 80. Ekstrom AD, Kahana MJ, Caplan JB, Fields TA, et al. Cellular networks underlying human spatial navigation. *Nature*. 2003; 425 (6954): 184-8. <https://doi.org/10.1038/nature01964>
 81. Epstein RA, Graham KS, Downing PE. Viewpoint-specific scene representations in human parahippocampal cortex. *Neuron*. 2003; 37 (5): 865-76. [https://doi.org/10.1016/S0896-6273\(03\)00117-X](https://doi.org/10.1016/S0896-6273(03)00117-X)
 82. Epstein R, DeYoe EA, Press DZ, Rosen AC, Kanwisher N. The parahippocampal place area: recognition, navigation, or encoding? *Neuron*. 1999; 23 (1): 115-25. [https://doi.org/10.1016/S0896-6273\(00\)80758-8](https://doi.org/10.1016/S0896-6273(00)80758-8)
 83. Epstein R, Kanwisher N. A cortical representation of the local visual environment. *Nature*. 1998; 392 (6676): 598-601. <https://doi.org/10.1038/33402>
 84. Park S, Chun MM. Different roles of the parahippocampal place area (PPA) and retrosplenial cortex (RSC) in panoramic scene perception. *Neuroimage*. 2009; 47 (4): 1747-56. <https://doi.org/10.1016/j.neuroimage.2009.04.058>
 85. Stevens WD, Kahn I, Wig GS, Schacter DL. Hemispheric asymmetry of visual scene processing in the human brain: evidence from repetition priming and intrinsic activity. *Cereb Cortex*. 2012; 22 (8): 1935-49. <https://doi.org/10.1093/cercor/bhr273>
 86. Rajimehr R, Devaney KJ, Bilenko NY, Young JC, Tootell RB. The "parahippocampal place area" responds preferentially to high spatial frequencies in humans and monkeys. *PLoS Biol*. 2011; 9 (4): e1000608. <https://doi.org/10.1371/journal.pbio.1000608>